

Work function and image-plane position of metal surfaces

P. A. Serena, J. M. Soler, and N. García

Departamento de Física de la Materia Condensada, C-III, Universidad Autónoma de Madrid, Cantoblanco, E-28049 Madrid, Spain

(Received 30 November 1987)

We present fully-self-consistent calculations of the electron density in some characteristic simple-metal surfaces. We obtain exact numerical results for the electron density using local pseudopotentials averaged in the directions parallel to the surface and very-thick-slab geometries. The resulting work functions considerably improve the agreement between experiment and perturbative results. Our results show that the distance of the image plane to the first atomic layer depends only weakly on the crystallographic orientation of the surface, in marked contrast with the strong dependence predicted from the jellium model.

The density-functional formalism^{1,2} has constituted a powerful tool³ for the study of the electronic structure and fundamental properties of many systems.⁴ This theory has been shown to be specially useful in the study of the metallic surface.⁵ Using this scheme, good quantitative results have been obtained for the electronic-charge-density profile in the surface region, the surface electrostatic dipole, the work function, the surface energy, potential barriers, the image-plane position, etc.

In this work we will continue the precursory studies of Lang and Kohn⁶⁻⁸ on several properties of metal surfaces. In their work they used the well-known jellium model in which the ionic point charges are replaced by a semi-infinite distribution of constant positive charge. They used the local-density approximation⁴ (LDA) for describing exchange and correlation effects and the calculations were worked out self-consistently by solving the Kohn-Sham equations.² With this simple model they found very significant behavior of the negative-charge density near the metallic surface region. To introduce the influence of the periodic lattice on several surface magnitudes, Lang and Kohn used first-order perturbation theory. In this way, they analyzed the lattice effects on the surface energy⁶ and the work function.⁷ Later on, several authors have studied the dependence of the work function⁹ and the surface energy¹⁰ on the crystallographic face using parametric variational methods. In these studies the electron density is calculated using a simple parametrized potential for better representing the ionic structure. Suitable values for these potential parameters are obtained by minimization of the total energy of the metal using the true potential. These parametric variational calculations improve considerably the results obtained by perturbation theory applied to the jellium model.

In this work we have solved self-consistently the Kohn-Sham equations including in a total way a local ionic pseudopotential within the self-consistent procedure. Therefore we do not have recourse either to parametric variational techniques or to perturbative methods. For describing the interaction between one ion and one electron, we use the local empty-core pseudopotential proposed by Ashcroft:¹¹

$$\begin{aligned} V_{ps}(\mathbf{r}) &= 0, & r < r_c \\ V_{ps}(\mathbf{r}) &= -Z_i/r, & r \geq r_c \end{aligned} \quad (1)$$

where Z_i represents the ionic charge and r_c is a cutoff radius which has been determined to give a good description of the largest number of bulk properties of each metal. The r_c values that we have chosen in the present work are the same used by Lang and Kohn in their calculations.^{6,7} The self-consistent solution of the initial three-dimensional problem is very complex and, for avoiding long and costly calculation methods, we will assume that the variation of the different physical magnitudes along the directions parallel to the metal surface is not important with regard to the change of these magnitudes along the normal direction. Then, at each point \mathbf{r} , we can replace the electron density and the different potentials by their average over the plane which contains \mathbf{r} and, at the same time, is parallel to the metal surface, so that now any physical magnitude will depend only on z , the coordinate perpendicular to the metal surface. This turns the three-dimensional calculation into a one-dimensional problem.

Our calculation needs four input parameters for describing the metal-vacuum interface: first, r_s , which is related to the mean electron density n_{av} of the bulk metal via the equation $\frac{4}{3}\pi r_s^3 = 1/n_{av}$; second, Z_i , the electrostatic charge of each metal ion; third, r_c , the pseudopotential cutoff radius; and finally d , the distance between two consecutive atomic planes which are parallel to the metal surface we wish to study.

The introduction of ionic pseudopotentials within the self-consistent procedure causes new problems in solving the Schrödinger equation within the Kohn-Sham equation system. In the jellium model, both the effective potential $v_{eff}(\mathbf{r})$ and the electron density $n(\mathbf{r})$ take constant values far inside the bulk, therefore it is possible to treat the electronic wave functions as plane waves asymptotically within the metal and then the advisable system to be studied is a semi-infinite jellium. With a pseudopotential, it is necessary to solve previously the bulk band structure and the asymptotic behavior of the Friedel oscillations becomes considerably more complicated. To develop the

calculation under these circumstances we assume that the electronic structure of metal can be studied by means of a metallic slab. In this way the problem is reduced to calculate the eigenstates of the effective-potential quantum well associated to the metallic slab. The quantum-size effects, which have an influence on work function,¹² density of states (DOS) and Fermi level,¹³ are diminished by choosing of a thick enough slab. Although the calculation requires long computation times and the convergence process is more difficult, we have found that this procedure is the most practical one. In our work the slab thickness is usually about 160 a.u. This means that, for example, we handle 37 layers for representing the (111) aluminum face or 60 layers for the (110) face of the same metal. Exchange-correlation effects are included in the mono-electronic effective potential $v_{\text{eff}}(\mathbf{r})$ by means of the local-density approximation, following the interpolation form due to Wigner.¹⁴ One of the limitations of this approximation is the failure to reproduce the characteristic behavior of classical image potential $-1/4z$ outside the metal surfaces. But the influence of this external shape on properties such as work function or surface energy is negligible.⁶ This is because of the very small electron density placed in regions where the image-potential effect becomes important.

Figure 1 shows the effective potential $v_{\text{eff}}(z)$ and the electron-density profile $n(z)$ for Al(111) and Li(100) faces. The first thing to notice is that the oscillations in $n(z)$ due to the periodic pseudopotential are considerably larger than the Friedel oscillations. This can be noticed because of the coincidence of the maxima of $n(z)$ with the minima of effective potential. Since the Friedel oscillations are themselves important in some cases to determine the electrostatic surface dipole and work function, it should be expected that a self-consistent treatment of the response to the pseudopotential is also important to determine these quantities.

In the jellium model it can be shown⁶ that, to ensure charge neutrality, the jellium edge must be fixed at the midpoint between the last plane of ions and the position of the first missing plane. Since the electron-density profile depends only on the position of the jellium edge, the distance between the density drop and the last plane of ions depends strictly linearly on the interplanar distance d . Figure 2 shows the electron-density profile for three faces of Al compared with that of the jellium model (with the jellium edge placed as we have explained above in each case). The interesting point to notice is that the density obtained with the pseudopotential drops at an approximately constant distance from the last plane of ions, nearly independent of the interplanar separation. Thus, the jellium model predicts a density drop which is too far for compact faces (large interplanar distance) and too close for open ones.

The influence on bcc-metal density profiles, such as Li, Na, etc., is similar to that one noticed for fcc metals, but taking into account that (110) and (111) faces are the closest configurations for bcc and fcc crystallographic structures, respectively. The density profile most similar to that obtained from the jellium model is that one corresponding to (100) planes, both for bcc and fcc metals. If

we compare our calculation of the electron-density profile of the Li(100) face to the planar average of the electron density evaluated by Alldredge and Kleinman,¹⁵ we notice that the exponential decay is very similar in both works. However, the bulk oscillation amplitude obtained by them doubles approximately the value we have calculated here and their first peak is more pronounced. These differences are originated partly by their use of a thinner 13-layer (100) film of lithium and partly by the difference in the pseudopotential employed (they use a nonlocal, but energy-independent, pseudopotential). If we compare our results for the Al(111) face to the calculation of Chelikowsky *et al.*,¹⁶ which was carried out using self-consistent pseudopotentials and a 12-layer slab, we notice that the bulk oscillation we have found is now more pronounced for the effective potential as well as for the elec-

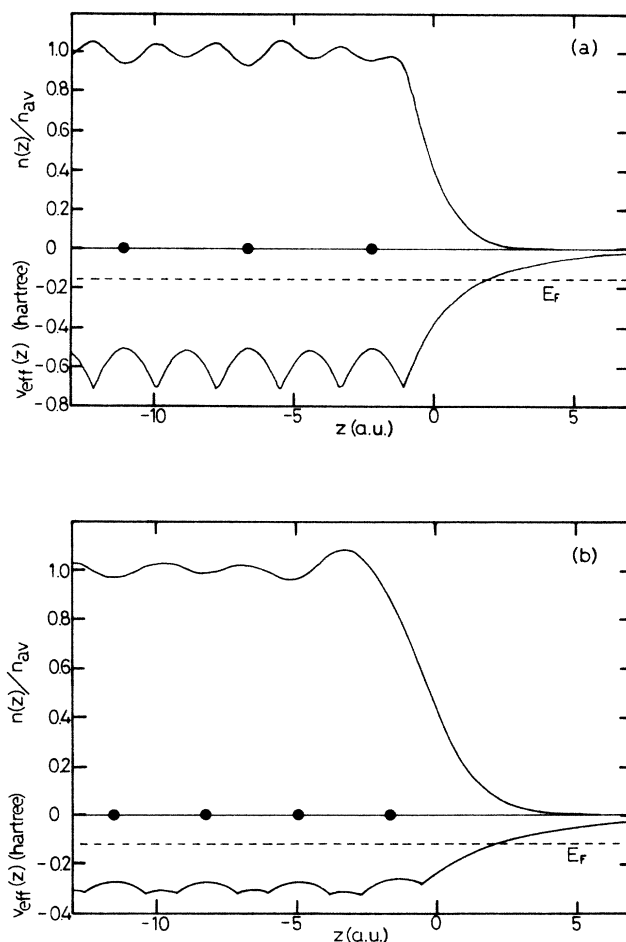


FIG. 1. Self-consistent electronic-charge density $n(z)$ and effective one-electron potential $v_{\text{eff}}(z)$, for (a) Al(111) and (b) Li(100) faces. The charge density is given in units of n_{av} , the mean electron density of the bulk metal. Black circles represent the position of the atomic planes. Dashed line represents the Fermi level. The position $z = 0$ is separated from the last atomic layer by half an interlayer spacing, $d/2$.

tron density. Nevertheless, they have calculated a maximum peak near the surface in accord with the trend observed on the Li(100) calculation of Alldredge and Kleinman.¹⁵ In both cases, our study gives main peaks more

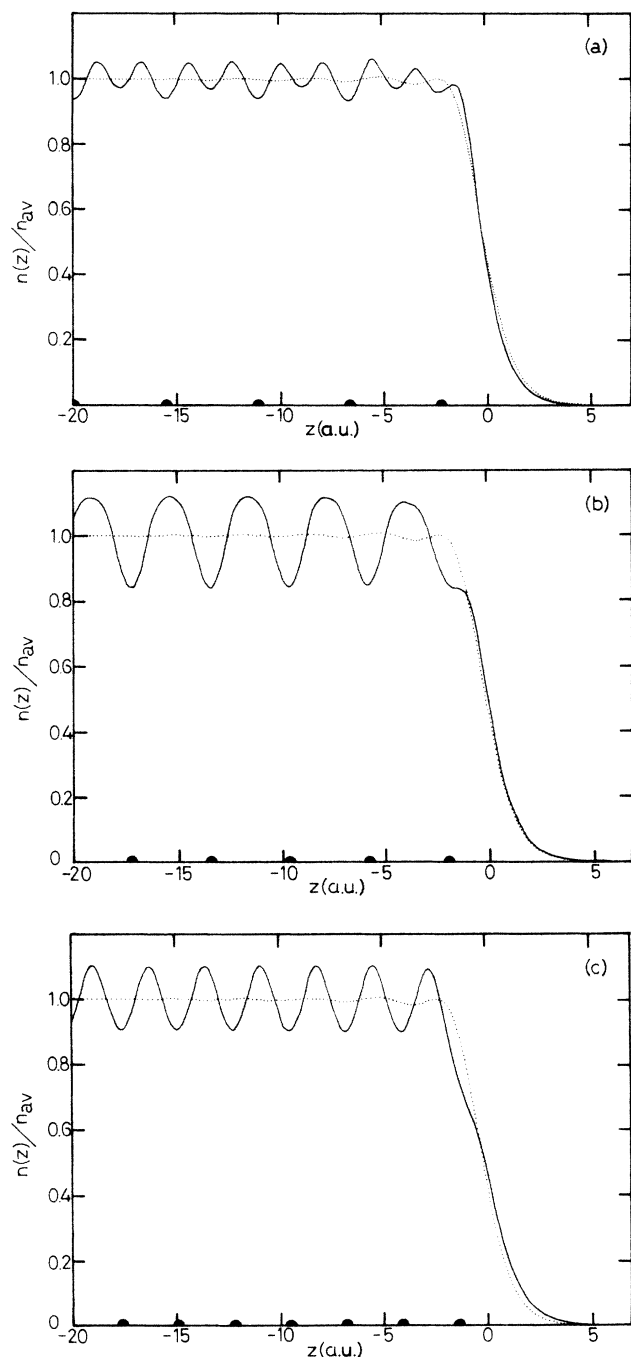


FIG. 2. Self-consistent electronic-charge density $n(z)$ for (a) (111), (b) (100), and (c) (110) faces of Aluminum. Solid curves represent the results obtained using local averaged pseudopotentials (present work) and dotted curves represent the electron density obtained using the jellium model (Ref. 6). Solid semicircles represent the position of the atomic planes.

reduced, similar to those obtained from the jellium metal.⁶ We can infer that the pseudopotential choice affects basically the bulk electron-density oscillation and first Friedel peak, but outside the metal the exponential-decay behavior is less pseudopotential dependent. However, we must draw attention to the overestimate of almost 20% in the work function of Al(111) by Chelikowsky *et al.*¹⁶ in comparison with experimental data.^{17,18}

Below we analyze the dependence of the work function Φ on the crystallographic face. The work-function anisotropy is closely linked to the dipole moment created by electron density and the positive ionic charge of the last few atomic planes.¹⁹ Up to now the work-function calculation has been carried out from several points of view.²⁰ Those studies that replace the original metal by one-dimensional models, as extensions of work of Lang and Kohn,⁶ have introduced the pseudopotential effects using either first-order perturbation theory⁷ or a parametric variational method.⁹ Here we have introduced the ionic lattice fully self-consistently using planar averaged pseudopotentials. In Table I we compare our work-function values for (111), (100), and (110) faces of several metals with bcc structure (Li, Na, Cs) and fcc structure (Al, Pb) with those of other calculations and also we show some experimental results.^{17,18,21–24} It is important to remark that the nonperturbative results represent a great improvement over those obtained perturbatively⁷ for metals in which the ionic pseudopotential is large [see, for instance, Al(111) and Al(110)]. On the contrary, metals with a small oscillation of ionic pseudopotential certainly permit a perturbative calculation (see Cs work function). Results which have been obtained from the change-in-the-self-consistent-field theory⁹ (a variational method), present a great agreement with ours for Na, but they disagree somewhat in the cases of Pb and Al. None of these one-dimensional models, including ours, explain well the work function of metals in which d orbitals play an important role. For instance, our work-function calculation on Ag and Cu gives values 25% below experimental data. General arguments¹⁹ suggest that the work function should increase with the compactness of the surface. However, for lead and aluminum our calculated work functions show the anomalous trend $\Phi_{100} > \Phi_{111}$, which has been noticed previously for some measurements¹⁸ and also in the calculations of Lang and Kohn.⁷ Nevertheless, the magnitude of this anomalous behavior is considerably reduced with respect to that in perturbative results.⁷ The agreement among our theoretical results and experimental data is excellent for the most densely packed surfaces of Al and Pb. For open faces the Φ values are lower than those found experimentally. It might be thought that this behavior could be due to the relaxation of the position of the last few atomic planes, which has been studied widely both experimentally²⁵ and theoretically.²⁶ In a previous work,²⁷ we have taken in account the surface relaxation using the ionic pseudopotential in the same way as in this study. We have shown that the work function changes less than 1% when the experimental relaxation displacements²⁵ are introduced. Therefore we think that our one-dimensional model is not very accurate for describing open crystallographic faces

TABLE I. Theoretical work function in eV for the three low-index planes of five simple metals, obtained using first-order perturbation theory (Ref. 7), parametric variational calculations (Ref. 9), and local averaged pseudopotentials within the self-consistent procedure (present work). Also we include experimental results.

Metal	Face	Work function (eV)				
		Ref. 7	Ref. 9	Present work	Experiment	
Li	(110)	3.55	3.55	3.63	2.93 ^a	
	(100)	3.30	3.32	3.32	(polycrystalline)	
	(111)	3.25	3.13	3.19		
Na	(110)	3.10	3.13	3.11	2.75 ^b	
	(100)	2.75	2.84	2.88	(polycrystalline)	
	(111)	2.65	2.76	2.76		
Cs	(110)	2.60		2.62	2.14 ^c	
	(100)	2.30		2.36	(polycrystalline)	
	(111)	2.20		2.24		
Al	(111)	4.05	4.27	4.18	4.26 ^d	4.24 ^e
	(100)	4.20	4.25	4.27	4.20 ^d	4.41 ^e
	(110)	3.65	4.02	3.88	4.06 ^d	4.28 ^e
Pb	(111)	4.15		4.30	4.25 ^f	
	(100)	4.50	4.10	4.31	(polycrystalline)	
	(110)	3.80	3.90	3.98		

^aReference 21.

^bReference 22.

^cReference 23.

^dReference 17.

^eReference 18.

^fReference 24.

where both electron density and potentials have an appreciable variation along the directions parallel to the metal surface. Nevertheless, the discrepancy among different experimental data for Al(110) and Al(100) work functions^{17,18} and the absence of data on the work-function anisotropy of Pb make necessary more measurements to settle this point.

Another issue of increasing interest in the last few years is the location of the image plane. Calculations on image-plane position have been carried out starting from the jellium model. Lang and Kohn⁸ have shown rigorously that the image plane is located at the centroid of the excess charge induced by a uniform electric field perpendicular to the metal surface. They themselves obtained the shape of the induced-charge density $\delta n(z)$ and the image-plane position z_0^{jel} (referred to the jellium edge) which represents the effective metal face.⁶ Within their calculation they used the LDA for describing the exchange-correlation potential and they did not take into consideration that this approach does not reproduce the expected $-1/4z$ asymptotic behavior of the image potential. Recent calculations try to correct this deficiency, including in some way the nonlocal effects within the exchange-correlation potential. On the one hand, Ossicini *et al.*²⁸ calculate the position of centroid within the framework of the weighted-density (WD) approximation.²⁹ On the other hand, we have calculated³⁰ electron

densities, effective potentials and the image-plane location z_0 at a jellium surface using the LDA inside the metal and a physically based interpolation to the classical image potential outside. Results for z_0^{jel} , reached using these two methods show only a slight contraction with respect to the purely LD calculation.⁸ Other methods³¹ have obtained z_0^{jel} values from the asymptotic behavior of the WD exchange-correlation potential far outside the metal surface, but this scheme seems to establish artificially the image-plane position.

In earlier studies the distance between the image plane and the last atomic layer is a magnitude which is usually underestimated. In the jellium treatment, this separation, d_{im} , is given by the simple expression

$$d_{\text{im}} = z_0^{\text{jel}} + d/2 . \quad (2)$$

This is because the jellium edge is separated from the last atomic layer by half an interlayer spacing, that is, $d/2$. It is easy to notice the large dependence of d_{im} on the crystallographic face when the jellium model is taken into account. The d_{im} change between the most and the least faces we have studied, that is, $|d_{\text{im}(111)} - d_{\text{im}(110)}|$, is 0.86 a.u. for Al, 1.04 a.u. for Pb, and 1.38 a.u. for Li. This strong variation is given only by the $d/2$ contribution since z_0^{jel} is a constant for each metal. In this work

we attempt to describe the influence of the crystallographic face on image-plane position in a more reliable way than formula (2). We calculate d_{im} as the centroid position of the charge $\delta n(z)$ by an electric field perpendicular to the metal surface. But now, the induced electron density is calculated rather than the jellium model using the planar-averaged pseudopotentials within the self-consistent procedure. In this way d_{im} is calculated directly from $\delta n(z)$ without any assumption about the position of the jellium edge. Induced-charge density profiles have a similar shape to those drawn by Lang and Kohn,^{7,8} appearing as a damped oscillation towards the metal inside and an induced-charge peak outside the metal, over the region where the centroid is located. The amplitude of this inner oscillation takes higher values for low-density metals. The outside peak is higher and narrower for high-density metals.

It is known that the image-plane position depends on the intensity of the applied electric field.³² To give a unique value of d_{im} we use that one obtained when the electric field tends towards zero. This forces us to do very accurate calculations to work with the lowest induced charges. Another possibility is to use both positive and negative electric fields and interpolate d_{im} to zero field. We have checked that both procedures give the same result.

In a previous work,³⁰ we noticed that the image-plane position z_0 can be determined very accurately from the semiempirical relation

$$V'_{\text{xc}}(z_0)/V_{\text{xc}}(z_0)^2 \approx 1.8, \quad (3)$$

where $V_{\text{xc}}(z)$ is the exchange-correlation potential of the unperturbed system, within the LDA. This method circumvents the need of studying the response of the surface electron density to a weak applied electric field. In Fig. 3 we present the image-plane position for (111), (110), and (100) faces of Al and Li with respect to the last atomic layer. We show the d_{im} values obtained from Eq. (2), from the exact determination of the centroid of $\delta n(z)$ in the system including planar-averaged pseudopotentials, and from applying Eq. (3) to the same system. The difference between the last two methods is always less than ≈ 0.1 a.u., thus confirming our previous results with the jellium model⁸ and the validity of Eq. (3) in a wide variety of systems. The most important point to notice in Fig. 3 is that the determination of d_{im} through the jellium model greatly overestimates the dependence of d_{im} on interlayer distance, i.e., the crystallographic structure of the studied surface. In fact this dependence is even inverted in Al surfaces (we have noticed also this behavior in Pb). This overestimation is in qualitative agreement with the previous observation of a marked difference in the position of the density drop between the simple jellium and the pseudopotential systems (Fig. 2).

Thus, the jellium model overestimates the image-plane distance d_{im} by more than 0.4 a.u. in Al(111) and Li(110). This has important applications on several fields, such as the determination of surface image states,³³ the calculation of effective potential barriers for scanning tunneling

microscopy³⁴ (STM) or for calculating metal-semiconductor barriers.³⁵ In an earlier work,³⁶ we have used also this model for studying the adsorption of alkali atoms with great atomic radius on metal surfaces and we showed the importance of d_{im} value to determine surface dipoles and work-function changes at low coverages limit.

In conclusion, we have presented completely self-consistent calculations of the electron density in the surface region of some characteristic *s-p* metals, using local pseudopotential averaged over the planes parallel to the surface. The resulting work functions improve considerably the agreement with experiments in comparison with the perturbative results⁷ and agree roughly with previous

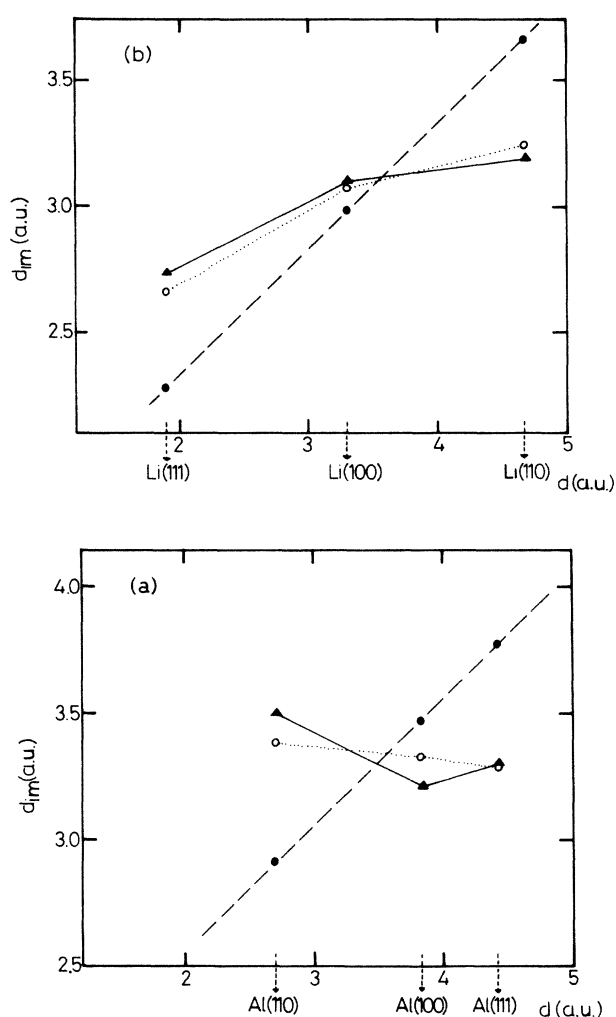


FIG. 3. Distance between the image plane and the last atomic layer, d_{im} , for (111), (100), and (110) faces of (a) aluminum and (b) lithium. We show the d_{im} values calculated from the exact determination of the centroid of $\delta n(z)$ including planar-averaged pseudopotentials (solid triangles), semiempirical relation of Eq. (3) (open circles), and the jellium model [Eq. (2)] (solid circles). The abscissa represents the interlayer spacing d . Different lines denote the behavior of d_{im} noticed from the three calculations.

values obtained with parametric variational methods.⁹ The calculated distance of the image plane to the last ion layer is only weakly dependent on the interlayer distance, in sharp contrast with the strong dependence predicted

from the jellium model. A previously proposed equation [Eq. (3)] for the determination of the image-plane position is neatly confirmed.

-
- ¹P. Hohenberg and W. Kohn, *Phys. Rev.* **136**, B864 (1964).
²W. Kohn and L. J. Sham, *Phys. Rev.* **140**, A1133 (1965).
³*Theory of the Inhomogeneous Electron Gas*, edited by S. Lundqvist and N. H. March (Plenum, New York, 1983).
⁴A. R. Williams and U. von Barth, in *Theory of the Inhomogeneous Electron Gas*, Ref. 3, and references therein.
⁵N. D. Lang, in *Theory of the Inhomogeneous Electron Gas*, Ref. 3, and references therein.
⁶N. D. Lang and W. Kohn, *Phys. Rev. B* **1**, 4555 (1970).
⁷N. D. Lang and W. Kohn, *Phys. Rev. B* **3**, 1215 (1971).
⁸N. D. Lang and W. Kohn, *Phys. Rev. B* **7**, 3541 (1973).
⁹R. Monnier, J. P. Perdew, D. C. Langreth, and J. W. Wilkins, *Phys. Rev. B* **18**, 656 (1978).
¹⁰J. P. Perdew and R. Monnier, *Phys. Rev. Lett.* **37**, 1286 (1976).
¹¹N. W. Ashcroft, *Phys. Lett.* **23**, 48 (1966).
¹²F. K. Schulte, *Surf. Sci.* **55**, 427 (1976).
¹³J. P. Rogers III, P. H. Cutler, T. E. Feuchtwang, and A. A. Lucas, *Surf. Sci.* **181**, 436 (1987).
¹⁴E. P. Wigner, *Phys. Rev.* **46**, 1002 (1934).
¹⁵G. P. Alldredge and L. Kleinman, *Phys. Rev. B* **10**, 559 (1974).
¹⁶J. R. Chelikowsky, M. Schlüter, S. G. Louie, and M. L. Cohen, *Solid State Commun.* **17**, 1103 (1975).
¹⁷R. M. Eastman and C. H. B. Mee, *J. Phys. F*, **3**, 1738 (1973).
¹⁸J. K. Grepstad, P. O. Gartland, and B. J. Slagsvold, *Surf. Sci.* **57**, 348 (1976).
¹⁹Smoluchowski, *Phys. Rev.* **60**, 661 (1941).
²⁰J. Hölzl and F. K. Schulte, in *Solid Surface Physics*, edited by G. Höhler (Springer-Verlag, Berlin, 1979), Vol. 85, p. 1.
²¹A. P. Ovchinnikov and B. M. Tsarev, *Fiz. Tverd. Tela (Leningrad)* **9**, 3512 (1967) [*Sov. Phys.—Solid State* **9**, 2766 (1968)].
²²R. J. Whitefield and J. J. Brady, *Phys. Rev. Lett.* **26**, 380 (1971).
²³G. A. Boutry and H. Dormont, *Philips Tech. Rev.* **30**, 225 (1969).
²⁴D. E. Eastman, *Phys. Rev. B* **2**, 1 (1970).
²⁵J. R. Noonan and H. L. Davis, *Phys. Rev. B* **29**, 4349 (1984).
²⁶P. Jiang, P. M. Marcus, and F. Jona, *Solid State Commun.* **59**, 275 (1986).
²⁷P. A. Serena and N. García, *Surf. Sci.* **189/190**, 232 (1987).
²⁸S. Ossicini, F. Finocchi, and C. M. Bertoni, *Surf. Sci.* **189/190**, 776 (1987).
²⁹O. Gunnarsson and R. O. Jones, *Phys. Scr.* **21**, 394 (1980); O. Gunnarsson, M. Jonson, and B. I. Lundqvist, *Phys. Rev. B* **20**, 3136 (1979).
³⁰P. A. Serena, J. M. Soler, and N. García, *Phys. Rev. B* **34**, 6767 (1986).
³¹S. Ossicini, C. M. Bertoni, and P. Gies, *Europhys. Lett.* **1**, 661 (1986); P. Gies, *J. Phys. C* **19**, L209 (1986).
³²W. Schmickler and D. Henderson, *Phys. Rev. B* **30**, 3081 (1984); P. Gies and R. R. Gerhardt, *Phys. Rev. B* **33**, 982 (1986).
³³D. Straub and F. J. Himpsel, *Phys. Rev. B* **33**, 2256 (1986); F. J. Himpsel, *Adv. Phys.* **32**, 1 (1983); G. Borstel and G. Thörner, *Surf. Sci. Rep.* **8**, 1 (1987).
³⁴G. Binnig, N. García, H. Rohrer, J. M. Soler, and F. Flores, *Phys. Rev. B* **30**, 4816 (1984).
³⁵I. P. Batra and S. Ciraci, *Phys. Rev. B* **33**, 4312 (1986).
³⁶P. A. Serena, J. M. Soler, N. García, and I. P. Batra, *Phys. Rev. B* **36**, 3452 (1987).